Molecular Therapy
Oncolytics
Original Article

Protein Palmitoylation Regulates Cell Survival by Modulating XBP1 Activity in Glioblastoma Multiforme

Xueran Chen,[1,2,7] Hao Li,[3,7] Xiaoqing Fan,[4,5] Chenggang Zhao,[1,3] Kaiqin Ye,[1,2] Zhiyang Zhao,[1,3] Lizhu Hu,[1,3] Huihui Ma,[6] Hongzhi Wang,[1,2] and Zhiyou Fang[1,2]

[1]Anhui Province Key Laboratory of Medical Physics and Technology, Center of Medical Physics and Technology, Hefei Institutes of Physical Science, Chinese Academy of Sciences, No. 350, Shushan Hu Road, Hefei, Anhui 230031, China; [2]Department of Molecular Pathology, Hefei Cancer Hospital, Chinese Academy of Sciences, No. 350, ShuShan Hu Road, Hefei, Anhui 230031, China; [3]School of Life Sciences, University of Science and Technology of China, No. 96, JinZhai Road, Hefei, Anhui 230026, China; [4]The First Affiliated Hospital of USTC, Division of Life Sciences and Medicine, University of Science and Technology of China (USTC), No. 17, Lujiang Road, Hefei, Anhui 230001, China; [5]Department of Anesthesiology, Anhui Provincial Hospital, No. 17, Lujiang Road, Hefei, Anhui 230001, China; [6]Department of Radiation Oncology, First Affiliated Hospital, Anhui Medical University, No. 218, JiXi Road, Hefei, Anhui 230031, China

Glioblastoma multiforme (GBM) almost invariably acquires an invasive phenotype, resulting in limited therapeutic options. Protein palmitoylation markedly affects tumorigenesis and malignant progression in GBM. The role of protein palmitoylation in GBM, however, has not been systematically reported. This study aimed to investigate the effect of protein palmitoylation on GBM cell survival and the cell cycle. In this study, most palmitoyltransferases were upregulated in GBM and its cell lines, and protein palmitoylation participated in signaling pathways controlling cell survival and the GBM cell cycle. Inhibition of protein palmitoylation with substrate-analog inhibitors, that is, 2-bromopalmitate, cerulenin, and tunicamycin, induced G_2 cell cycle arrest and cell death in GBM cells through enhanced endoplasmic reticulum (ER) stress. These effects are primarily attributed to the palmitoylation inhibitors activating pro-apoptotic pathways and ER stress signals. Further analysis revealed was the accumulation of SUMOylated XBP1 (X-box binding protein 1) and its transcriptional repression, along with a reduction in XBP1 palmitoylation. Taken together, the present results indicate that protein palmitoylation plays an important role in the survival of GBM cells, further providing a potential therapeutic strategy for GBM.

INTRODUCTION

Glioblastoma multiforme (GBM) is considered the most common type of intracranial tumor.[1,2] Despite improvements in conventional surgical, radiotherapy, and chemotherapy, the median survival of GBM patients is only approximately 14 months.[3,4] Thus, new therapeutic strategies or drugs targeting GBM are urgently needed.

Disturbances in endoplasmic reticulum (ER) homeostasis activate the ER stress response, which is mediated by three parallel signaling pathways initiated by protein kinase R-like ER kinase (PERK), inositol-requiring enzyme 1α (IRE1α), and activating transcription factor-6 (ATF6).[5,6] X-box binding protein 1 (XBP1) is a key transcription factor in the IRE1α signaling branch.[7,8] Upon ER stress, the XBP1 transcript is spliced by the endoribonuclease, IRE1α, to generate the active form, spliced XBP1 (XBP1s), which regulates genes implicated in protein folding, trafficking, and secretion, thus enhancing cell survival and ER homeostasis under ER stress. In contrast, unspliced XBP1 (XBP1u) functions as the dominant negative form antagonizing the function of XBP1s.[9,10] Furthermore, IRE1α serves as a kinase to activate pro-apoptotic c-Jun N-terminal kinase (JNK) signaling to induce cell death.[11,12] The seemingly paradoxical dual functions of IREα in inducing both pro-survival and pro-apoptotic signaling upon ER stress is challenging to understand.

Protein functions are influenced by their expression level, localization, interaction with other proteins, and posttranslational modifications.[13–15] Numerous proteins can be modified through palmitoylation at cysteine residues by a family of enzymes containing a unique DHHC domain.[16,17] At least 23 members of this palmitoyltransferase (PAT) family have been reported in the mammalian genome. Protein localization, trafficking, and stability are regulated by this modification.[18,19] Palmitoylation markedly influences tumorigenesis and tumor progression through different substrates, particularly in glioma development and malignant progression.[20,21] For example, ZDHHC5

Received 12 March 2020; accepted 20 May 2020;
https://doi.org/10.1016/j.omto.2020.05.007.

[7]These authors contributed equally to this work.

Correspondence: Xueran Chen, Anhui Province Key Laboratory of Medical Physics and Technology, Center of Medical Physics and Technology, Hefei Institutes of Physical Science, Chinese Academy of Sciences, No. 350, Shushan Hu Road, Hefei, Anhui 230031, China.
E-mail: xueranchen@cmpt.ac.cn
Correspondence: Zhiyou Fang, Anhui Province Key Laboratory of Medical Physics and Technology, Center of Medical Physics and Technology, Hefei Institutes of Physical Science, Chinese Academy of Sciences, No. 350, Shushan Hu Road, Hefei, Anhui 230031, China.
E-mail: z.fang@cmpt.ac.cn

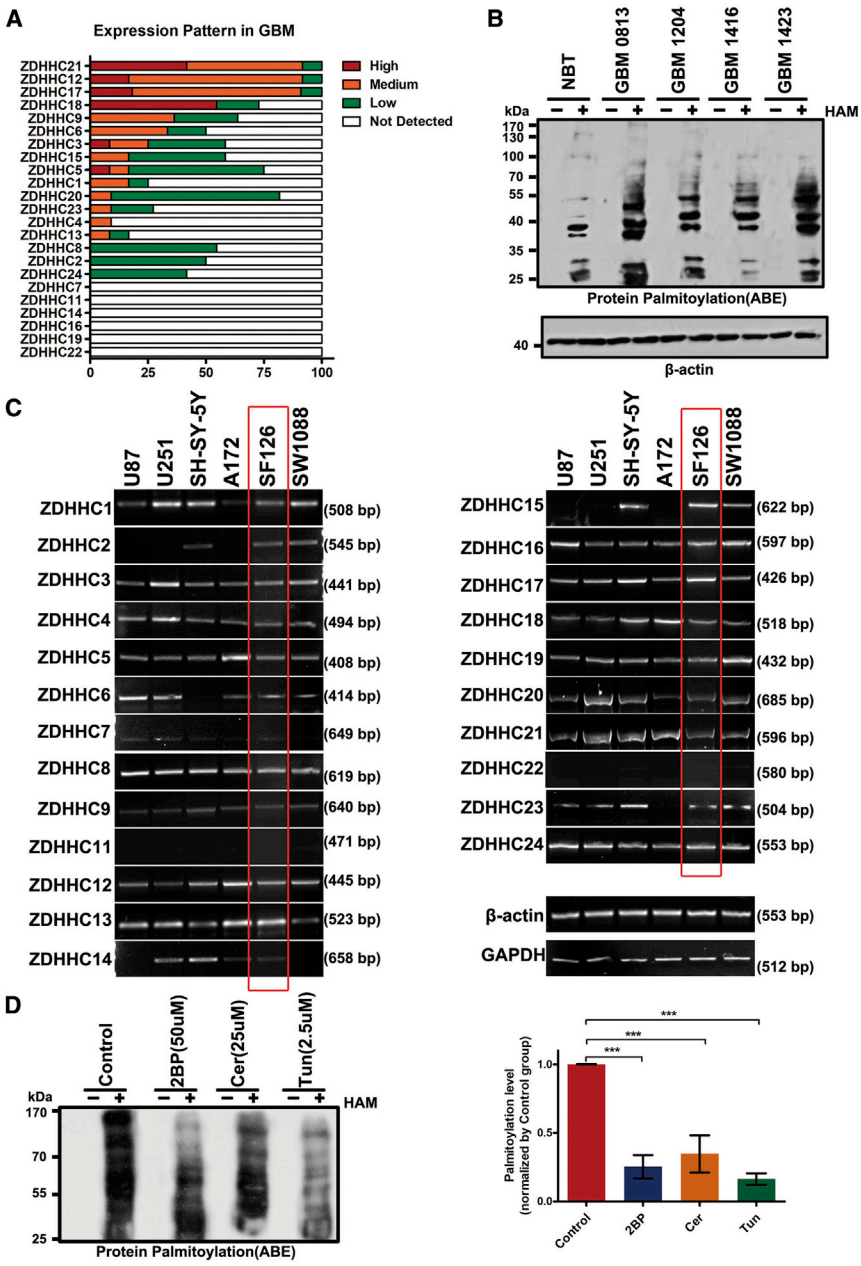

Figure 1. Expression of Palmitoyltransferases (PATs) and Protein Palmitoylation in Glioblastoma Multiforme (GBM) Cells

(A) The expression of different DHHCs in GBM is summarized on the basis of immunohistochemical findings of the Human Protein Atlas. (B) Acyl-biotin exchange (ABE) detection of the palmitoylated proteins in normal brain tissue (NBT) and GBM tissues. HAM+, hydroxylamine-treated sample; HAM−, Tris-treated control (no hydroxylamine). (C) Reverse transcription polymerase chain reaction (RT-PCR) analysis of the mRNA levels of the 23 known PATs in six GBM cell lines. β-Actin and GAPDH were used as controls. (D) 2-Bromopalmitate (2BP; 50 μM), cerulenin (Cer; 25 μM), and tunicamycin (Tun; 2.5 μM) inhibited protein palmitoylation in SF126cells. ***$p < 0.001$, unpaired t test.

is upregulated in p53 mutant glioma cells and enhances their invasiveness and tumorigenicity.[22] Moreover, ZDHHC23 and ZDHHC18 contribute to the transition of glioma stem cells and cell survival in a stressful tumor microenvironment.[23] Thus, palmitoylation inhibitors would potentially be effective for treating GBM.

2-Bromopalmitate (2BP), which irreversibly inhibits PATs, is the most commonly used palmitoylation inhibitor.[24] Two additional important lipid-based DHHC inhibitors are cerulenin (Cer) and tunicamycin (Tun).[25] In the present study, we initially analyzed the expression pattern of DHHC members in GBM and investigated the effect of protein palmitoylation on GBM cell survival and the cell cycle.

RESULTS

Protein Palmitoylation Occurs in GBM and Cell Lines

To determine the role of protein palmitoylation in GBM pathogenesis and malignant progression, we initially evaluated the expression of the 23 potential PATs in GBM based on the Human Protein Atlas (Figure 1A). Most of the DHHC members were upregulated in GBM, especially for ZDHHC21, ZDHHC12, ZDHHC17, and ZDHHC18. We then quantified total protein palmitoylation via acyl-biotin exchange analyses. Compared to normal brain tissues, GBM displayed several protein bands with covalent palmitoyl modifications (Figure 1B). These results suggest that GBM involves changes in protein palmitoylation, and aberrant protein palmitoylation may be a potent biomarker for GBM.

Furthermore, we analyzed the expression of all DHHCs in six human GBM cell lines via RT-PCR (see Table S1 for primer sequences). Of the 23 PATs, 20 were detected in these six cell lines (Figure 1C). ZDHHC7, ZDHHC11, and ZDHHC22 were undetectable, suggesting that they were downregulated in GBM cells. In subsequent experiments, we used SF126 cells to investigate the roles of protein palmitoylation during GBM pathogenesis because the 20 PATs were most upregulated in this cell line. Consistent with the GBM tissues, some palmitoylated proteins were detected in SF126 cells (Figure 1D).

Inhibition of Protein Palmitoylation Causes GBM Cell Cycle Arrest and Apoptosis

To determine whether protein palmitoylation is involved in SF126 cell function, we inhibited palmitoylation with three PAT inhibitors,

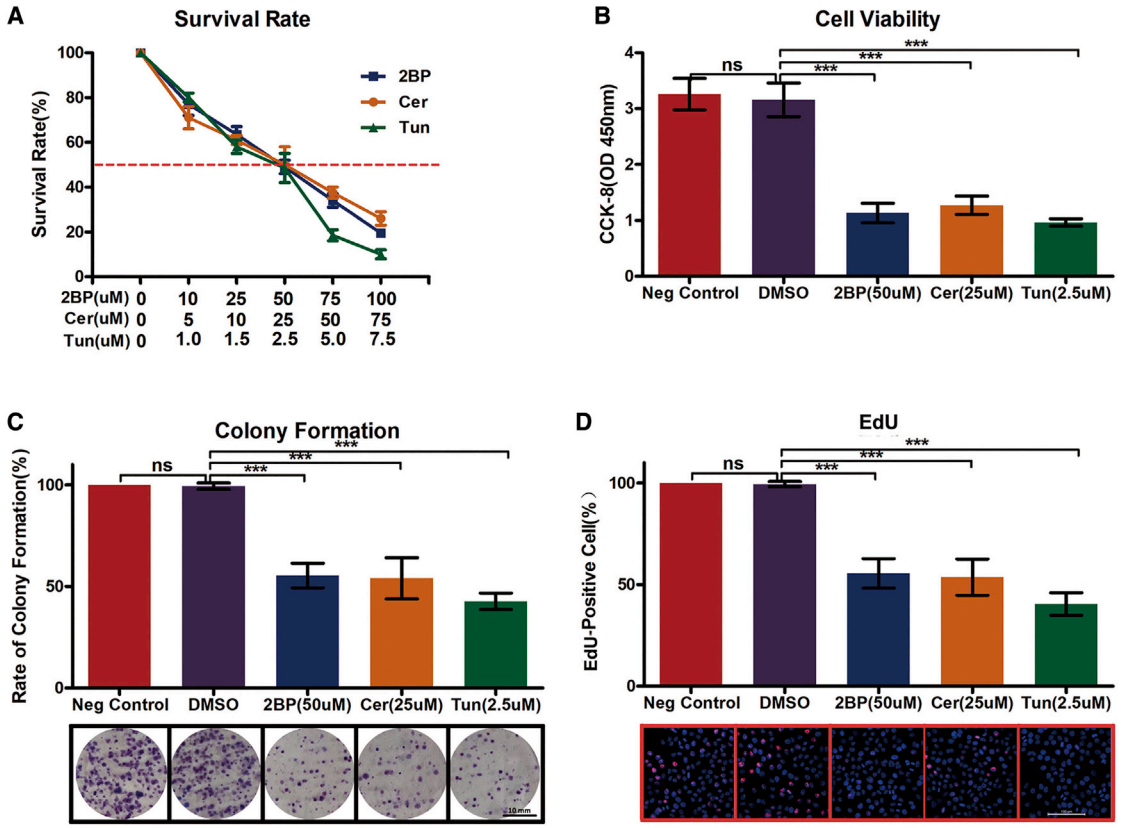

Figure 2. Inhibition of Palmitoylation-Repressed Cell Growth and Proliferation

(A) Palmitoylation inhibitors decrease cell survival of SF126 cells. SF126 cells were plated onto 96-well plates and treated with different concentrations of 2BP (50 μM), Cer (25 μM), or Tun (2.5 μM) for 48 h, followed by enumeration of surviving cells. (B) Palmitoylation inhibitors decreased SF126 cell viability. SF126 cells were plated onto 96-well plates and treated with 2BP (50 μM), Cer (25 μM), or Tun (2.5 μM) for 48 h, followed by the evaluation of cell viability using the CCK-8 assay. (C) Palmitoylation inhibitors decrease colony formation of SF126 cells. SF126 cells were plated onto 10-cm plates and treated with 2BP (50 μM), Cer (25 μM), or Tun (2.5 μM) for 2 weeks when the number of cell colonies was determined. Scale bar, 10 μm. (D) SF126 cells were treated with 2BP (50 μM), Cer (25 μM), or Tun (2.5 μM) for 48 h, and cell proliferation was assessed using the Edu assay. Scale bar, 100 μm. ***$p < 0.001$, unpaired t test. ns, not significant.

that is, 2BP, Cer, and Tun. Consequently, 50 μM 2BP, 25 μM Cer, and 2.5 μM Tun adequately repressed protein palmitoylation in glioma cells by 85%, 75%, and 65%, respectively (Figure 1D). EZH2 can be palmitoylated;[22] however, in this study, EZH2 palmitoylation levels were reduced after 2BP, Cer, or Tun treatment to different degrees (Figure S1A).

The effect of palmitoylation on cell survival was determined by using 2BP at 10–100 μM, Cer at 5–75 μM, and Tun at 1.0–7.5 μM in SF126 cells. Consequently, treatment with 50 μM 2BP, 25 μM Cer, and 2.5 μM Tun adequately decreased the cell survival rate by 50% (Figure 2A) and adequately decreased cell viability (Figure 2B), colony formation (Figure 2C), and cell proliferation (Figure 2D) among GBM cells. Thus, we used palmitoylation inhibitors at these concentrations in subsequent experiments.

To investigate the effects of protein palmitoylation on cell cycle progression, GBM cells were exposed to 2BP, Cer, and Tun for 48 h, and the cell cycle phase distribution was analyzed using fluorescence-activated cell sorting (Figures 3A–3C). Quantification of untreated SF126 cells revealed that 76.5% (76.5% for negative control; 75.1% for dimethyl sulfoxide [DMSO]) of the cells were in the G_0/G_1 phase, 7.27% (7.27% for negative control; 8.17% for DMSO) were in the S phase, and 14.8% (14.8% for negative control; 17.2% for DMSO) were in the G_2/M phase of the cell cycle 48 h after plating. Treatment of SF126 cells with 50 μM 2BP for 48 h increased the percentage of cells in the G_2/M phase to 62.8% and reduced cells in the G_0/G_1 and S phases to 11.8% and 4.96%, respectively. The sub-G_1 cell population exceeded 20.6%. The percentage of SF126 cells treated with 25 μM Cer for 48 h in the G_2/M phase increased to 52.0% and the sub-G_1 population of cells exceeded 16.1%. Tun (2.5 μM) increased the percentage of cells in the G_2/M phase to 25.0% and the sub-G_1 population of cells exceeded 29.0%. These data indicate that SF126 GBM cells underwent cell cycle arrest in the G_2/M phase upon treatment with 2BP, Cer, or Tun.

Furthermore, we performed annexin V-propidium iodide (PI) double staining with fluorescence-activated cell sorting to verify that SF126

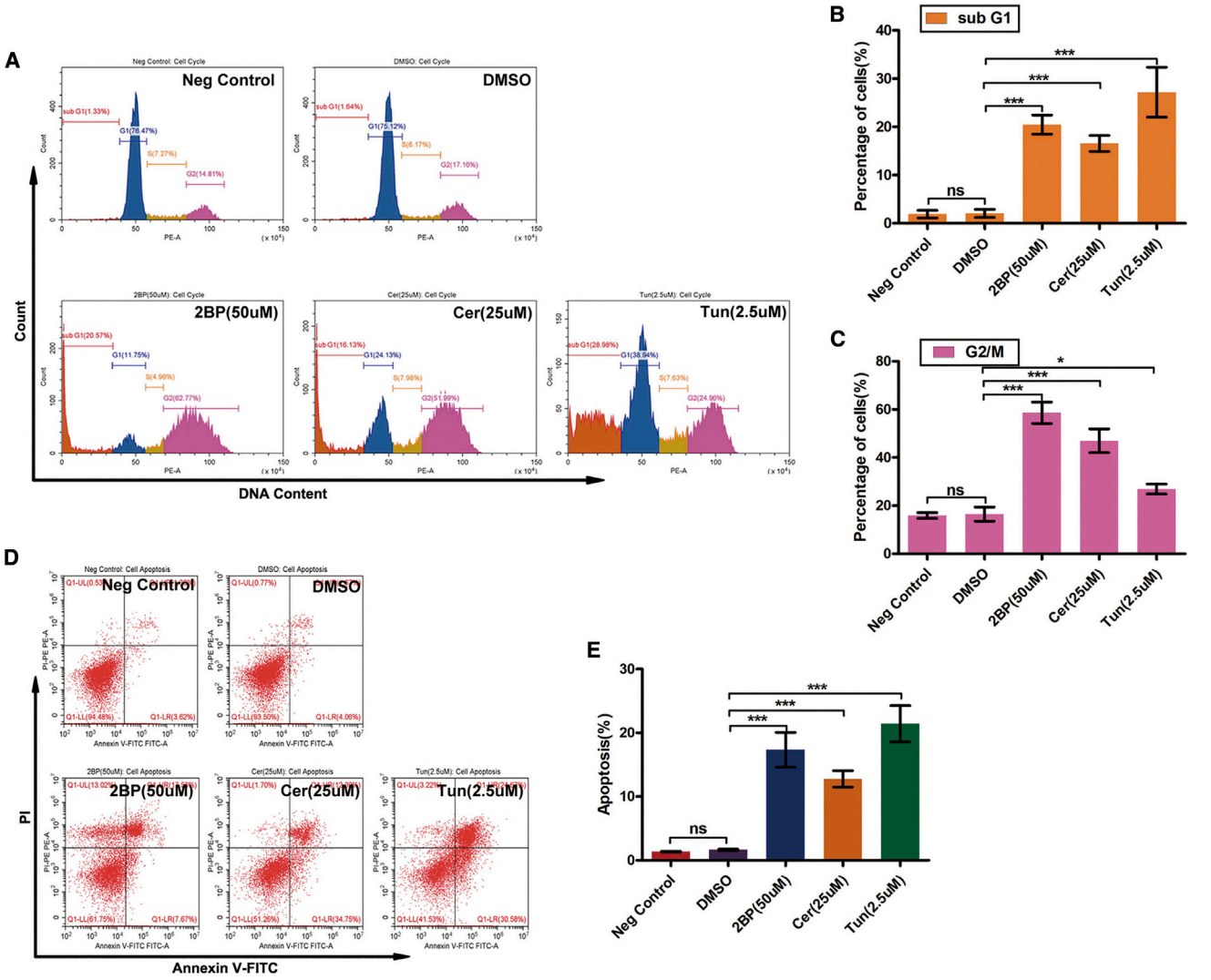

Figure 3. Inhibition of Palmitoylation Induces G_2 Cell Cycle Arrest and Cell Death

(A–C) Effects of palmitoylation inhibitors on the cell cycle. (A) SF126 cells were treated with 2BP (50 μM), Cer (25 μM), or Tun (2.5 μM) for 48 h, and then the cell cycle distribution was analyzed via flow cytometry. (B and C) The sub-G_1 (B) and G_2/M (C) cell populations were quantified. (D and E) Effect of palmitoylation inhibitors on apoptosis in SF126 cells. Cells were treated with 2BP (50 μM), Cer (25 μM), or Tun (2.5 μM) for 48 h and analyzed for apoptosis using annexin V-propidium iodide double staining and flow cytometry (D). The apoptotic cell population was quantified (E). *$p < 0.05$, ***$p < 0.001$, unpaired t test. ns, not significant.

GBM cells treated with palmitoylation inhibitors underwent apoptosis (Figure 3D). Control GBM cells exhibited a very low apoptotic rate (1.36% for negative control; 1.67% for DMSO). The apoptotic population increased significantly to 17.6% with 50 μM 2BP, 12.3% with 25 μM Cer, and 24.7% with 2.5 μM Tun (Figure 3E). These data indicate that apoptosis plays a role in palmitoylation inhibitor-induced cell death.

Transcriptomes Are Altered after Palmitoylation Inhibition

We performed RNA sequencing (RNA-seq) to investigate alterations in the transcriptome upon 2BP, Cer, and Tun treatment. On treating the SF126 GBM cell line with 50 μM 2BP, 433 genes were upregulated and 441 were downregulated in comparison with the control DMSO-treated cells. These upregulated genes were associated with biological processes, including responses to organic substances and carboxylic acid metabolic processes (Figure 4A). Upon treatment with 25 μM Cer, 488 genes were downregulated and 271 were upregulated in comparison with the DMSO control group. These upregulated genes were involved in responses to organic substances and ER stress (Figure 4B). Upon treatment with Tun (2.5 μM versus DMSO), 590 genes were upregulated and 833 genes were downregulated. These upregulated genes were involved in responses to ER stress and unfolded proteins (Figure 4C).

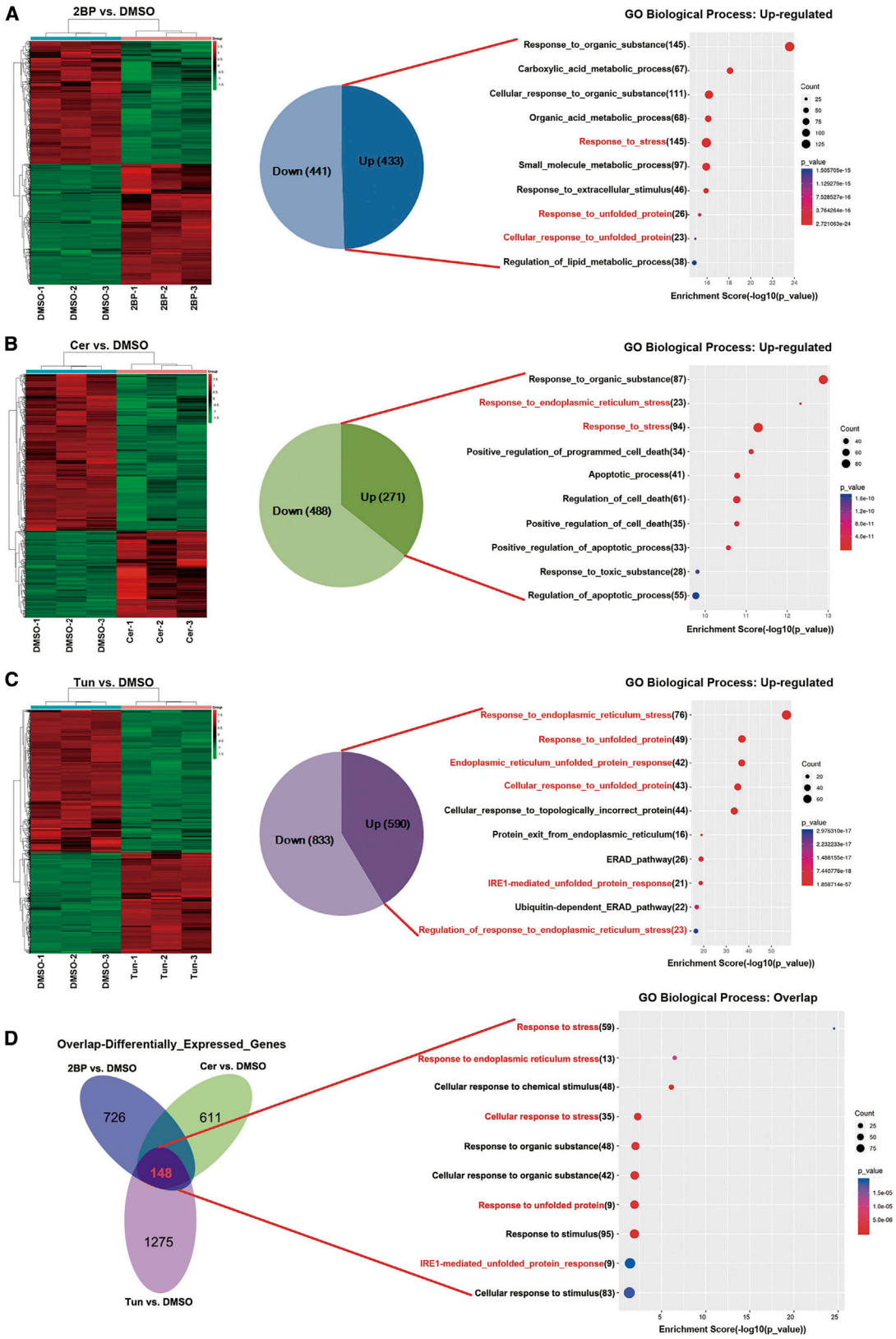

(legend on next page)

In total, 148 transcripts were differentially expressed in the 2BP versus DMSO, Cer versus DMSO, and Tun versus DMSO datasets. We performed a Gene Ontology analysis with respect to the biological process to determine the biological relevance of the 148 differentially expressed gene transcripts obtained from the aforementioned three RNA-seq datasets. Several biological processes were enriched in palmitoylation inhibitor-treated samples as opposed to untreated samples, primarily including responses to stress, ER stress, and chemical stimuli (Figure 4D). Taken together, these results indicate that inhibition of palmitoylation in GBM cells activates responses to ER stress, increases the levels of unfolded proteins, and causes other changes associated with ER stress.

Inhibition of Palmitoylation Triggers the Pro-apoptotic ER Stress Response

Most PATs were localized at the ER, Golgi, and in cytoplasmic vesicles (Figure 5A). PDI (protein disulfide isomerase) is an ER enzyme that catalyzes thiol-disulfide exchange, thus facilitating disulfide bond formation and rearrangement reactions.[26] Immunostaining revealed that PDI accumulated in cells treated with palmitoylation inhibitors, suggesting the occurrence of ER stress (Figure 5B). Consistent with these results, electron microscopy revealed progressive morphological changes in the ER after inhibition of palmitoylation, including swollen and abnormal areas (Figure 5C), directly indicating ER stress.

Because ER stress is one of the major cell stress responses associated with apoptosis, we investigated whether palmitoylation inhibitors activated the ER stress response, as well as its pro-apoptotic effects in GBM cells. As shown in Figure 6, treatment of SF126 cells with 2BP, Cer, or Tun increased IRE1α phosphorylation and, concurrently, IRE1α levels. Since IRE1α activation results in JNK activation,[11] herein JNK phosphorylation showed a similar time course pattern as IRE1α. Consistent with IRE1α phosphorylation, XBP1s protein levels significantly increased. On treatment with the anti-XBP1s antibody, XBP1u protein levels decreased.

The ER stress response of SF126 GBM cells exposed to 2BP, Cer, or Tun was also evidenced by the increase in CCAAT-enhancer binding protein homologous protein (CHOP) levels. Apoptosis in these cells was reflected by increased cleavage of caspase-3 (Figure 6). These results show that inhibition of palmitoylation induces the ER stress response, which correlates with palmitoylation inhibitor-induced apoptosis.

Inhibition of Palmitoylation Represses Pro-survival XBP1 Signaling

Having observed that 2BP, Cer, and Tun activate the ER stress response, we further assessed the effect of inhibition of palmitoylation on target mRNA (*XBP1*, *VEGFA*, *GADD34*, and *CHOP*) levels in these signaling pathways in GBM cells. Among these target genes, both *CHOP* and *GADD34* are regulated by non-IRE1α (PERK and ATF6) branches of the ER stress response.[27] Human VEGFA contains putative XBP1s that binds at sites in its promoter, and these sites are conserved across species, including mice, rats, and humans.[28] XBP1 is a downstream target of the XBP1s gene in positive feedback loops.[28] In the present study, 2BP, Cer, and Tun suppressed *XBP1* and *VEGFA* mRNAs in SF126 cells and potently induced *CHOP* and *GADD34* mRNAs (Figure 7A).

Furthermore, we used a 5× unfolded protein response element (UPRE) luciferase reporter construct to assess the transcriptional activity of XBP1s. Consequently, 2BP, Cer, and Tun treatment inhibited the relative luciferase activity of 5× UPRE that was induced by co-transfected XBP1s (Figure 7B). This finding indicates that palmitoylation inhibitors potentially inhibit the transcriptional activity of XBP1s selectively while enhancing the mRNA expression of downstream factors, as reflected via upregulation of *GADD34* and *CHOP* mRNAs (target genes of the non-IRE1α cascade ER stress response, such as the PERK/eIF2α signaling pathway) in GBM cells.

XBP1s levels were increased, whereas its transcriptional activity was repressed, after treatment with palmitoylation inhibitors. SUMOylation potentially suppresses the transcriptional activity of XBP1s during ER stress.[29] To test this possibility, we investigated whether SUMOylation of XBPs is increased in palmitoylation inhibitor-treated cells. As shown in Figure 7C, XBP1s SUMOylation was increased after 2BP, Cer, or Tun treatment in comparison with untreated cells, suggesting that reduction of protein palmitoylation specifically results in the accumulation of SUMOylated XBP1s. Indeed, an increase in SUMOylated XBP1s levels is potentially associated with the inhibition of palmitoylated XBP1s because palmitoylation levels of XBP1s were discernibly decreased upon treatment with 2BP, Cer, or Tun. As predicted using CSS-Palm 4.0, XBP1s has three potential palmitoylation sites at its C terminus: Cys325, Cys331, and Cys339. These potential palmitoylation sites are proximal to SUMOylation sites at XBP1s, that is, Lys281 and Lys302. Palmitoylation of XBP1s may hinder XBP1s SUMOylation. As assumed, mutations at the potential palmitoylation sites in XBP1s decreased XBP1s palmitoylation levels and increased the XBP1s SUMOylation levels (Figure 7D). Considering the interaction between a PAT and its substrate,

Figure 4. Transcriptomes in SF126 Cells Treated with Palmitoylation Inhibitors

(A–C) Heatmaps showing differentially expressed genes in SF126 cells treated with 2BP (A; 50 μM), Cer (B; 25 μM), or Tun (C; 2.5 μM) for 48 h. Euclidean distance was considered for row and column clustering. The color bars show the normalized effect of compounds on the gene expression levels (green indicates downregulated and red indicates upregulated) compared to cells treated with DMSO. Classification based on the biological process term on Gene Ontology analysis of upregulated mRNAs. (D) Venn diagrams showing the overlap of differentially expressed genes in the three treatment groups. Overlapping genes were generally classified on the basis of the biological process.

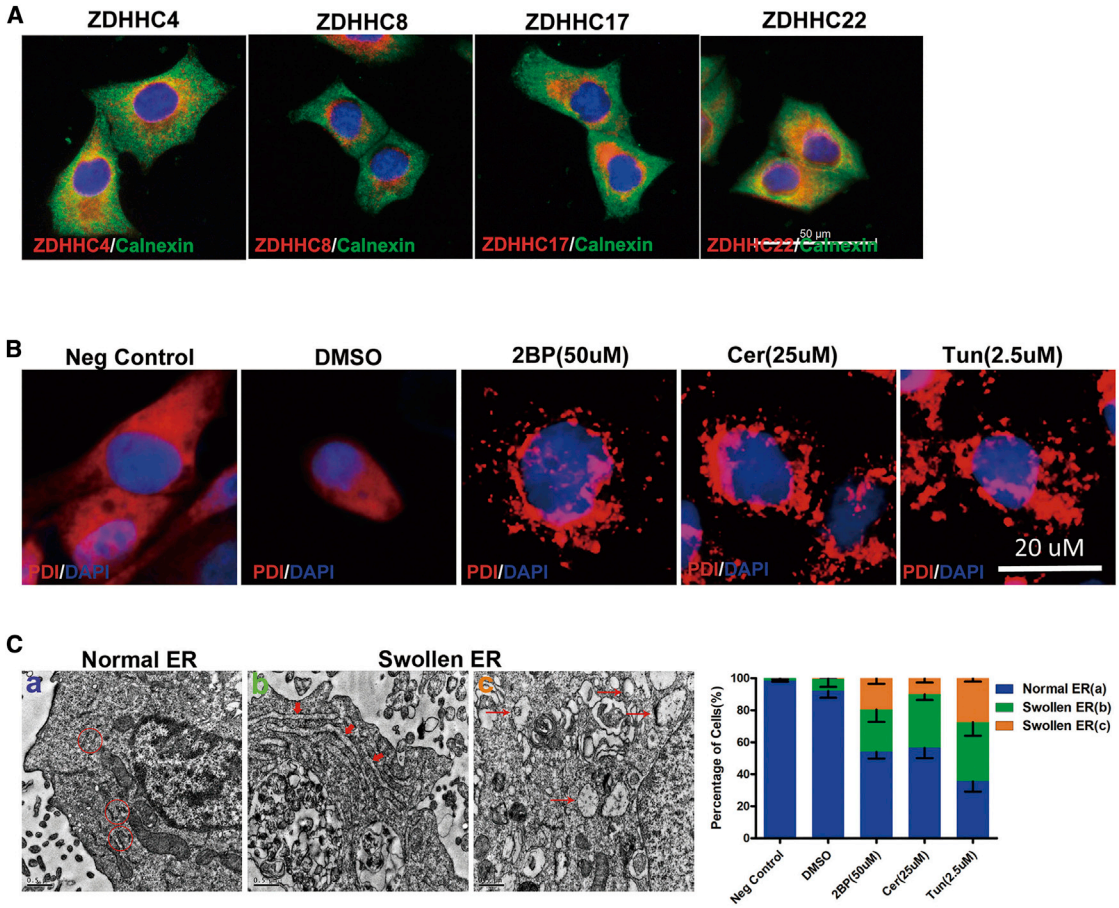

Figure 5. Inhibition of Palmitoylation Triggers Endoplasmic Reticulum (ER) Stress

(A) Localization of four DHHC proteins in SF126 cells. ZDHHC4, ZDHHC8, ZDHHC17, and ZDHHC22 (green) co-localize with the ER marker calnexin (red). Scale bar, 50 μm. (B) SF126 glioblastoma cells were treated with 2BP (50 μM), Cer (25 μM), or Tun (2.5 μM) for 48 h, and the cytoplasmic distribution of PDI (red) was observed via confocal microscopy. Scale bar, 20 μm. (C) Structural changes in the ER in SF126 cells treated with 2BP (50 μM), Cer (25 μM), or Tun (2.5 μM) for 48 h, and observed via transmission electron microscopy. Scale bars, 0.5 μm. n = 20.

we tested some DHHC members upregulated in GBM that may bind to XBP1s in SF126 cells. Co-immunoprecipitation analysis revealed the physical interaction between XBP1s and three DHHC members, that is, ZDHHC1, ZDHHC6, and ZDHHC17 (Figure 7E). Concurrently, knockdown of ZDHHC1, ZDHHC6, or ZDHHC17 resulted in a reduction in XBP1s palmitoylation but an increase in XBP1s SUMOylation (Figure 7F). These results suggest that XBP1s palmitoylation specifically inhibits XBP1s SUMOylation, and palmitoylation inhibitors can increase XBP1s SUMOylation and repress its transcriptional activity.

Treatment Prospects of Palmitoylation Inhibitors for GBM

In Vivo

Recently, radiotherapy and temozolomide (TMZ) chemotherapy treatments have become the gold standard treatment methods for GBM after surgery. We initially analyzed the expression of the 23 potential PATs in SF126 cells after treatment with X-ray irradiation (IR) and TMZ via RT-PCR (Figure S2). More interestingly, ZDHHC5 and ZDHHC8 were upregulated only in the IR-treated group (Figure S2A), suggesting that these PATs potentially contribute to this phenomenon. ZDHHC4/9/11/14/17/21/22/24 were upregulated only in the TMZ-treated group (Figure S2B), suggesting that these PATs potentially corroborate the effects of TMZ treatment. ZDHHC7 was upregulated in both IR- and TMZ-treated cells (Figure S2C). ZDHHC2 was upregulated after IR treatment but downregulated after TMZ treatment (Figure S2D). However, ZDHHC12/13/16/18/23 were slightly downregulated in the IR- or TMZ-treated cells rather than the untreated cells (Figure S2E), while ZDHHC1/3/6/15/19/20 levels remained unchanged (Figure S2F). These results indicate that PATs markedly participate in IR and TMZ treatments among GBM patients.

Moreover, palmitoylation inhibitors (2BP, Cer, or Tun) displayed cooperative effects with IR and TMZ and significantly repressed GBM cell proliferation (Figure 8A), migration (Figure 8B), and invasion (Figure 8C). A xenograft model was used to evaluate the *in vivo*

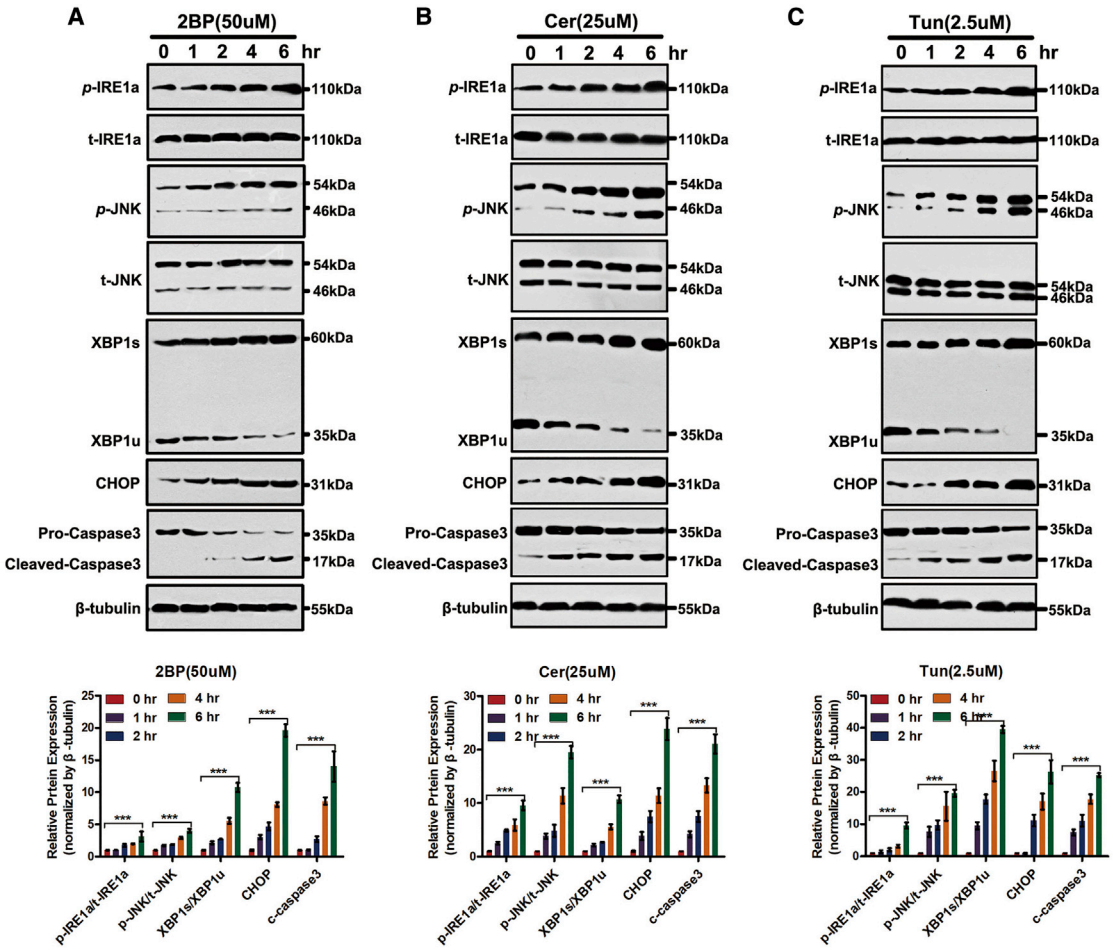

Figure 6. Inhibition of Palmitoylation Activates Inositol-Requiring Enzyme 1α (IRE1α) and Causes Death in SF126 Cells

(A–C) SF126 cells were treated with 2BP (50 μM; A), Cer (25 μM; B), or Tun (2.5 μM; C) for the indicated periods. Whole-cell lysates were harvested and analyzed for phosphorylated and total IRE1α, phosphorylated and total c-Jun N-terminal kinase (JNK), spliced (XBP1s) and unspliced X-box binding protein 1 (XBP1)u, CCAAT-enhancer binding protein homologous protein (CHOP), pro-caspase-3, cleaved caspase-3, and the loading control, β-tubulin. ***$p < 0.001$, unpaired t test.

anti-tumor activity of palmitoylation inhibitors. Approximately 1×10^6 SF126 cells were injected at the dorsa of nude mice. After tumors grew to approximately 100 mm^3, the mice (six animals per group) were subcutaneously administered 3 mg/kg 2BP, 5 mg/kg Cer, or 2 mg/kg Tun daily for 10 days, along with IR and TMZ treatment. Consequently, all three agents significantly inhibited tumor growth in comparison with untreated mice or the TMZ/IR treatment group (Figure 8D). Immunohistochemical assessment revealed that Ki-67 expression levels *in vivo* were lower in inhibitor-treated versus untreated mice or TMZ/IR-treated mice (Figure 8E). As expected, palmitoylation levels of XBP1s were decreased to different degrees (Figure S1B). The *in vivo* analysis highlighted treatment prospects via IR and TMX treatment for GBM patients.

DISCUSSION

The present results reveal a novel mechanism through which palmitoylation inhibitors (2BP, Cer, and Tun) induce cell death in GBM cells. These inhibitors activate ER stress signaling and its pro-apoptotic effects, while promoting SUMOylated XBP1 accumulation and inhibiting XBP1s-mediated transcription and pro-survival signaling during ER stress. These results suggest that palmitoylation inhibitors are potential pharmacotherapeutic candidates for GBM by subjecting GBM cells to double jeopardy, thereby skewing the ER stress response survival/apoptosis balance toward apoptosis.

Almost all DHHC family members are associated with human diseases, spanning neurological disorders to some cancers, through different substrates such as oncogenic Ras,[30] Hedgehog,[31] Wnt,[32] and epidermal growth factor receptor[33] proteins. Hence, palmitoylation inhibitors are potentially beneficial for treating some cancers. Well-established lipid-based palmitoylation inhibitors include 2BP, Tun, and Cer. Within cells, 2BP is metabolically incorporated as 2BP-coenzyme A (CoA) and inhibits PAT activity of all DHHCs that have been tested.[34,35] The mode of action for Tun is still unclear;

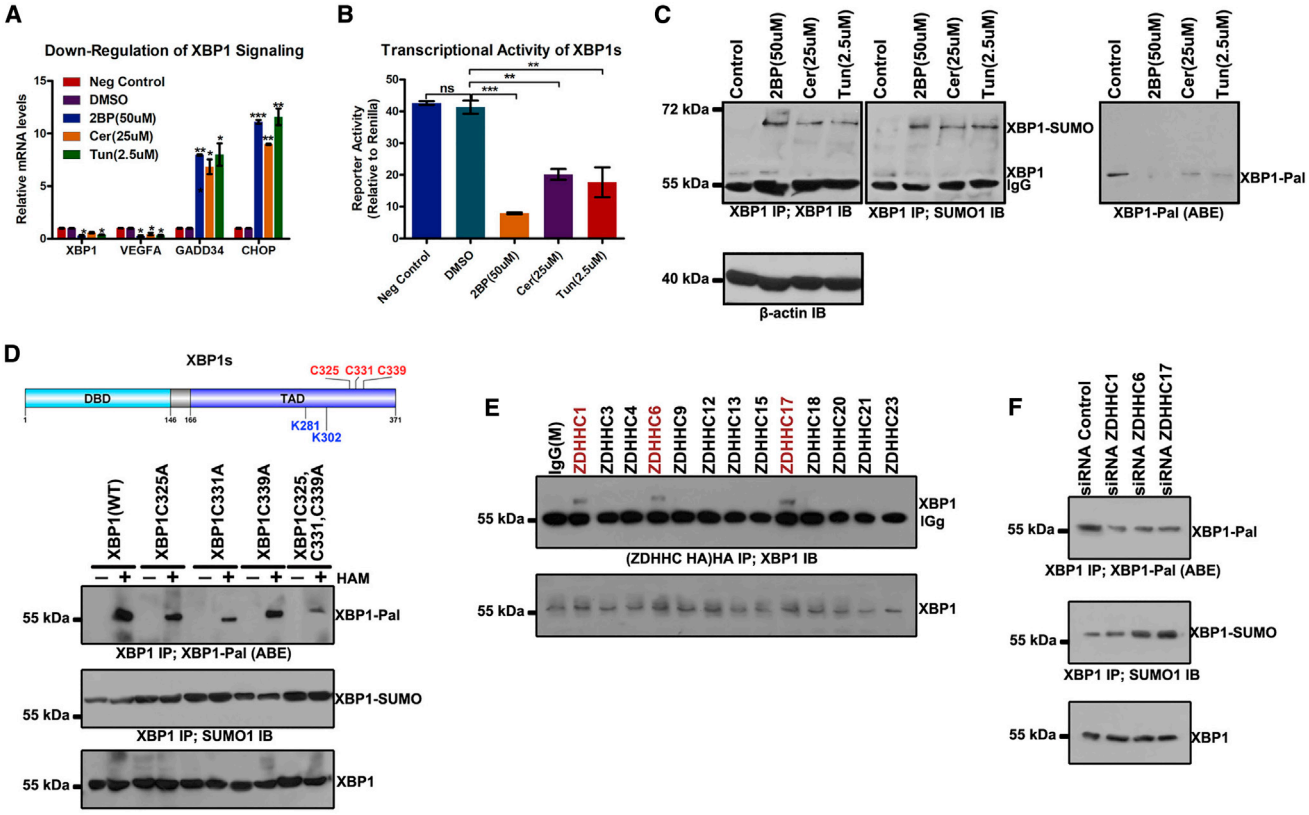

Figure 7. X-box Binding Protein 1 (XBP1) Signaling Is Downregulated by Palmitoylation Inhibitors in SF126 Cells

(A) SF126 cells were treated with 2BP (50 μM), Cer (25 μM), or Tun (2.5 μM) for 24 h. RNA was extracted from each sample and real-time polymerase chain reaction was performed to analyze the levels of spliced X-box binding protein 1 (XBP1s), vascular endothelial growth factor A (VEGFA), GADD34, and CCAAT-enhancer binding protein homologous protein (CHOP) mRNAs. (B) Palmitoylation inhibitors decreased the transcriptional activity of XBP1s. A 5× unfolded pathway response element-luciferase reporter and XBP1s expression construct were used to determine the transcriptional activity of XBP1s. The firefly luciferase value was divided by the Renilla luciferase value to normalize each sample. Data are expressed as means ± SD (n = 3). (C) Increased accumulation of SUMOylated XBP1 in 2BP (50 μM), Cer (25 μM), or Tun (2.5 μM) treatment versus that in control group. XBP1 was immunoprecipitated with anti-XBP1 antibody (IP) from these cell lysates. Bound proteins were blotted with anti-XBP1 or anti-SUMO1 antibody (IB). (D) Cys325, Cys331, and Cys339 were determined as XBP1 palmitoylation sites. Palmitoylation sites Cys325, Cys331, and Cys339 of XBP1 were predicted using CSS-Palm 4.0 and mutated to Ala, respectively, the palmitoylation level of XBP1 was detected via the ABE method, and the SUMOylated XBP1 was also analyzed. (E) SF126 was transfected with hemagglutinin (HA)-tagged DHHC members upregulated in GBM, and subjected to immunoprecipitation (IP) of HA. (F) Palmitoylation and SUMOylation levels of XBP1 in SF126 cells transfected with siRNAs for different DHHCs. *$p < 0.05$, **$p < 0.01$, ***$p < 0.001$, unpaired t test. ns, not significant.

however, it may compete with the palmitoyl-CoA substrate for binding to DHHC-PATs.[36] Cer is proposed to react irreversibly with the catalytic cysteine of DHHC, or cysteine residues of the substrate proteins, through its epoxy carboxamide group.[37] Protein palmitoylation significantly influences tumorigenesis and progression in GBM. Thus, we used these lipid-based palmitoylation inhibitors to assess the role of palmitoylation in GBM pathogenesis. Our results show that inhibition of protein palmitoylation with 2BP, Cer, or Tun induced GBM cell G_2 cell cycle arrest, increased cell death, and inhibited glioma growth. Regarding the regulation of GBM cell survival by protein palmitoylation, we found that inhibition of palmitoylation induces ER stress through the IRE1α/JNK/XBP1 signaling axis. IRE1α/JNK/XBP1 signals play both pro-apoptotic and pro-survival roles under stress conditions mediated by JNK and XBP1s, respectively.[38,39] XBP1s activates proteins regulating protein trafficking, folding, and quality control through the ER-associated protein degradation pathway.[40]

GBM is a solid tumor in cells that can survive hypoxia, nutrient deprivation, and low pH. Furthermore, Bip and PERK are upregulated in GBM cells,[41,42] suggesting an intrinsic dependence on the ER stress pathway for survival. The ER stress sensor IRE1α contributes to GBM progression through XBP1 mRNA that splices and regulates IRE1-dependent mRNA decay.[42] Interference with the ER stress pathway may affect cell survival. For example, pharmacologic inhibition of IRE1α endoribonuclease activity inhibits XBP1 mRNA splicing and decreases cellular sensitivity to ER stress-induced death. Bortezomib increases intrinsic ER stress in GBM cells by inducing the accumulation of numerous unfolded proteins and/or and blocking the degradation of misfolded proteins.[43] Bortezomib,

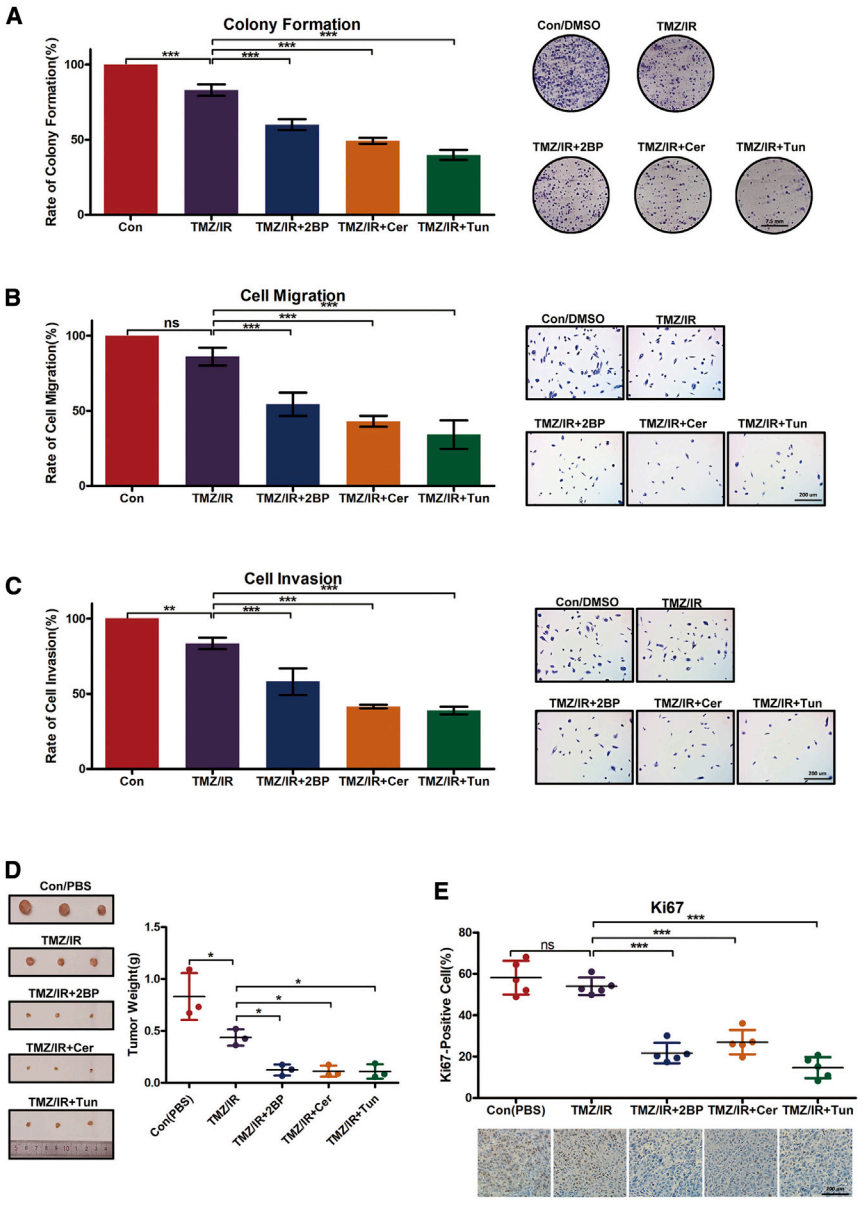

Figure 8. Inhibition of Palmitoylation Represses Malignancy Progress in GBM

(A) Palmitoylation inhibitors along with IR/TMZ significantly decrease colony formation among SF126 cells. SF126 cells were plated onto 10-cm plates and treated with IR (6 Gy), TMZ (200 μM), 2BP (50 μM), Cer (25 μM), or Tun (2.5 μM) for 2 weeks, when the number of cell colonies was determined. (B and C) Palmitoylation inhibitors along with IR/TMZ significantly decreased cell migration (B) and invasion (C) of SF126 cells. (D and E) Xenograft tumors. When the tumor volume approached 100 mm^3, nude mice were subcutaneously treated with 3 mg/kg 2BP, 5 mg/kg Cer, or 2 mg/kg Tun daily for 10 d, along with IR at 20 Gy (4.5–4.6 Gy/min) and gastric infusion of TMZ (50 mg/kg/day). The mice were then euthanized. (D) Dissected tumors and tumor weights. (E) Typical immunohistochemistry images for Ki-67 in tumors, and quantification of Ki-67-expressing cells. Scale bars, 200 μm. Data are expressed as means ± SD (n = 6). Con (PBS), control, phosphate-buffered saline. *p < 0.05, **p < 0.01, ***p < 0.001, unpaired t test. ns, not significant.

however, represses the function of XBP1s via elevations in XBP1u levels, the unspliced and transcriptionally inactive form of XBP1 that antagonizes the functions of XBP1s.[44] Furthermore, our results indicate a distinct mechanism through which palmitoylation inhibitors affect XBP1s signaling in GBM cells. The present results show that although 2BP, Cer, and Tun activated IRE1α activity and enhanced mRNA splicing of XBP1, these agents exerted a specific inhibitory effect on XBP1s transcriptional activity, paradoxically without elevating XBP1u, leading to a defective autoregulation loop for XBP1, wherein XBP1s regulated the expression of total XBP1s. This concept is supported by the reduction in total XBP1 mRNA levels despite an increase in XBP1s protein levels in GBM cells in response to palmitoylation inhibitor treatment. Furthermore, these inhibitors repressed mRNA levels of another XBP1s target gene, *VEGFA*. Taken together, these results suggest that inhibition of protein palmitoylation induces ER stress and inhibits XBP1s-inducible mRNAs, including *XBP1* and *VEGFA*, thus promoting apoptosis in GBM cells upon ER stress.

The present results show that accumulation of SUMOylated XBP1 and the repression of its transcriptional function were accompanied by a reduction in XBP1 palmitoylation. SUMOylation suppresses transcription through multiple mechanisms.[45] Co-repressors are recruited through transcription factors via SUMO-dependent interactions, serving as a potential mechanism contributing to transcriptional regulation via SUMO. SUMOylation of certain co-repressors affects their transcriptional repressor activity, thus serving as another potential mechanism underlying SUMO-dependent transcriptional repression.[45,46] However, the effects of palmitoylation on XBP1 SUMOylation and its transcriptional activity warrant further investigation.

In summary, the present results show that most DHHC members are upregulated in GBM and inhibition of palmitoylation results in G_2 cell cycle arrest and cell death. These effects are primarily attributed to the potential of palmitoylation inhibitors to activate ER stress signals and consequent pro-apoptotic effects. Further analysis revealed the accumulation of XBP1 SUMOylation and the suppression of its transcriptional function after treatment with palmitoylation inhibitors. Taken together, these results

show that palmitoylation inhibitors potentially help treat malignant GBM.

MATERIALS AND METHODS

Cell Lines and Chemical Reagents

Human GBM cell lines U87, U251, SH-SY-5Y, A172, SF126, and SW1088 were purchased from the American Type Culture Collection (Manassas, VA, USA) and characterized via DNA fingerprinting and isozyme detection. These cell lines were cultured in Dulbecco's modified Eagle's medium containing 10% fetal bovine serum (FBS) and 100 ng/mL of both penicillin and streptomycin. Cells were maintained at 37°C in a humidified atmosphere of 5% CO_2. All cultures were free of mycoplasma.

DMSO (D8418) and 2BP (21604) were purchased from Sigma-Aldrich (St. Louis, MO, USA). Cer (HY-A0210) and Tun (HY-A0098) were purchased from MedChemExpress (Monmouth Junction, NJ, USA). Anti-caspase-3 (9662), anti-cleaved caspase-3 (9661), anti-CHOP (2895), anti-JNK (9252), anti-phosphorylated (phospho-) JNK (9255), anti-IRE1α (3294), and anti-β-actin antibodies were purchased from Cell Signaling Technology (Danvers, MA, USA). The anti-phospho-IRE1α antibody (ab48187) was purchased from Abcam (Cambridge, MA, USA). The anti-XBP-1 antibody (sc-7160) was purchased from Santa Cruz Biotechnology (Santa Cruz, CA, USA).

Cell Viability Assay

Cells were seeded in 96-well plates at 4,000 cells per well and incubated overnight. Following treatment for 24 h, WST-8 reagent from Cell Counting Kit-8 (CCK-8; Beyotime Biotechnology, Haimen, China) was added to each well (final volume ratio was 10%). Absorbance was measured at 450 nm. All experiments were performed in triplicate.

EdU Assay

Cells were seeded in serum-free media overnight to allow for cell cycle synchronization and incubated with 5-ethynyl-2′-deoxyuridine (EdU; Cell-Light EdU Apollo 488 *in vitro* kit, Guangzhou RiboBio) for 2 h before fixation in 2% paraformaldehyde (PFA) and subsequent EdU detection per the manufacturer's protocol.

Cell Cycle Assay

The cell cycle status was assayed via PI staining using a Cytomics FC500 flow cytometer. The cell cycle profiles were determined using CXP analysis software (Beckman Coulter, Brea, CA, USA).

Apoptosis Assay

Cells were harvested via centrifugation and stained with annexin V and PI (V13242, Invitrogen, Carlsbad, CA, USA) in accordance with the manufacturer's instructions. Apoptotic cells were quantified via flow cytometry.

Transwell Migration and Invasion Assays

Transwell chambers with 8-μm pores (Corning Life Sciences) were utilized to assess cell migration. The Transwell membrane was previously coated with Matrigel matrix (30 μL) for the invasion assay of tumor cells (1:3 mixed with PBS; BD Biosciences). Cells (1×10^5) were loaded to the top chamber of the Transwell dish (8-μm pore size; Corning Life Sciences). FBS (10%) was loaded in the bottom chamber as a chemoattractant. In the bottom chamber, the cells were fixed and then stained with 0.005% (w/v) crystal violet. The number of invaded or migrated cells was measured by counting those five random areas in every membrane.

RNA Isolation, Real-Time PCR, and Sequencing

RNA was isolated from each cell sample using TRIzol (Invitrogen) in accordance with the manufacturer's instructions. Total RNA quality and quantity were verified using a NanoDrop 2000 spectrometer (Thermo Scientific, Rockford, IL, USA).

Transcript levels were determined via quantitative real-time PCR with iQ SYBR Green supermix (Bio-Rad, Hercules, CA, USA) and performed with a qTOWER 2.0 thermal cycler (Analytik Jena, Jena, Germany). Amplification conditions were as follows: 95°C for 3 min and then 95°C for 15 s, 55°C for 15 s, and 72°C for 30 s for 40 cycles. Primers used for this study were synthesized by Invitrogen and are enlisted in Table S1.

The Bioconductor RNA-seq workflow was followed to detect differential gene expression using DESeq 2 software and other Bioconductor packages in R.

Western Blot Analyses

Cells were rinsed twice with ice-cold phosphate-buffered saline and harvested by scraping into 100 μL of radio immunoprecipitation assay buffer, followed by rocking at 4°C for 30 min. The cell lysates were then centrifuged at 14,000 × *g* for 20 min at 4°C. Protein concentrations in the supernatants were quantified using a bicinchoninic acid protein assay kit. Using SDS-PAGE, proteins (50 μg) were resolved and then electrotransferred onto a polyvinylidene fluoride membrane. The membrane was blocked with 5% non-fat milk for 1 h and probed with the respective primary antibodies overnight at 4°C. The membrane was then washed three times with Tris-buffered saline/0.1% Tween 20 and probed with appropriate secondary antibodies for 1 h. An enhanced chemiluminescence detection system was used in accordance with the manufacturer's instructions.

Palmitoylation Assay

Cell lysates were prepared in the presence of 10 mM *N*-ethylmaleimide (23030, Pierce, Carlsbad, CA, USA), followed by denaturation with chloroform/methanol. Samples were further incubated overnight with 10 mM *N*-ethylmaleimide. After extensive washing with chloroform/methanol, samples were treated with hydroxylamine (HAM). After each chloroform/methanol precipitation, protein pellets were dissolved in aqueous buffers via sonication. After washing, HPDP-biotin (A35390, Pierce) was used for sulfhydryl biotinylation. Biotin-exchanged samples were affinity purified using the NeutrAvidin resin (53151, Pierce). Purified proteins were eluted by boiling in nonreducing SDS-PAGE loading buffer and detected

with horseradish peroxidase-conjugated NeutrAvidin, or with dithiothreitol for antibody-based detection.

Electron Microscopy

For electron microscopy, cells treated with 2BP, Cer, or Tun were harvested via centrifugation and fixed with 2% PFA and 3% glutaraldehyde for 1 h at room temperature. The fixed cells were harvested via centrifugation, washed three times with PBS, and incubated in PBS solution overnight at 4°C. Thereafter, the cells were post-fixed in 1% OsO_4 (pH 7.4) for 2 h at room temperature, dehydrated using an ascending ethanol series, and infiltrated with 100% acetone/resin (1:5) overnight at room temperature. Thereafter, cells were embedded in fresh resin and polymerized at 55°C for 1 h. Cut sections were supported on grids (150 nm), and the slides were stained with uranyl acetate for 15 min and lead citrate for 10 min at room temperature. Images were captured using JEM-1200EX transmission electron microscope (Japan Electron Optics Laboratory, Tokyo, Japan).

Tumor Xenograft Model

Experiments were carried out using 6- to 8-week-old C57BL/6 mice weighing 22–28 g. When the tumor volume approached 100 mm^3, the animals were randomly segregated into four groups: control, TMZ/IR, TMZ/IR+2BP, TMZ/IR+Cer, and TMZ/IR+Tun. Each group comprised six mice on day 0. These mice were treated (IR) with 20 Gy (4.5–4.6 Gy/min) for tumor induction and administered by gastric infusion with TMZ (50 mg/kg/day). 2BP (3 mg/kg), Cer (5 mg/kg), and Tun (2 mg/kg), dissolved in DMSO, were subcutaneously administered daily (distal from the sites of tumor inoculation) from days 0 to 10. The control group was treated with DMSO (or PBS) only. All animal experiments were approved by the Institutional Animal Care and Use Committee at Hefei Institutes of Physical Science, Chinese Academy of Sciences.

Statistical Analyses

A Student's t test was performed for all quantitative data between different groups. Statistical significance is indicated as $*p < 0.05$, $**p < 0.01$, and $***p < 0.001$. All quantitative data are presented as means ± SD from at least three independent experiments.

SUPPLEMENTAL INFORMATION

Supplemental Information can be found online at https://doi.org/10.1016/j.omto.2020.05.007.

AUTHOR CONTRIBUTIONS

Conception and design: X.C., H.W., and Z.F. Acquisition of data: H.L., X.F., C.Z., Z.Z., and L.H. Analysis and interpretation of data: X.C., K.Y., H.W., and H.M. Writing, review, and/or revision of the manuscript: X.C., X.F., and Z.F. Administrative, technical, or material support: L.H. and H.M. Study supervision: X.C. and K.Y. All authors read and approved the final manuscript.

CONFLICTS OF INTEREST

The authors declare no competing interests.

ACKNOWLEDGMENTS

This research was supported by the National Natural Science Foundation of China (81872066, 31571433, 81773131, and 81972635), the Innovative Program of Development Foundation of Hefei Center for Physical Science and Technology (2018CXFX004 and 2017FXCX008), the CASHIPS Director's Fund (YZJJ201704), and the Youth Innovation Promotion Association of the Chinese Academy of Sciences (2018487).

REFERENCES

1. Lee, E., Yong, R.L., Paddison, P., and Zhu, J. (2018). Comparison of glioblastoma (GBM) molecular classification methods. Semin. Cancer Biol. *53*, 201–211.
2. McFaline-Figueroa, J.R., and Lee, E.Q. (2018). Brain tumors. Am. J. Med. *131*, 874–882.
3. Jain, K.K. (2018). A critical overview of targeted therapies for glioblastoma. Front. Oncol. *8*, 419.
4. Lieberman, F. (2017). Glioblastoma update: molecular biology, diagnosis, treatment, response assessment, and translational clinical trials. F1000Res. *6*, 1892.
5. Almanza, A., Carlesso, A., Chintha, C., Creedican, S., Doultsinos, D., Leuzzi, B., Luís, A., McCarthy, N., Montibeller, L., More, S., et al. (2019). Endoplasmic reticulum stress signalling—from basic mechanisms to clinical applications. FEBS J. *286*, 241–278.
6. Hiramatsu, N., Chiang, W.C., Kurt, T.D., Sigurdson, C.J., and Lin, J.H. (2015). Multiple mechanisms of unfolded protein response-induced cell death. Am. J. Pathol. *185*, 1800–1808.
7. Jiang, D., Niwa, M., and Koong, A.C. (2015). Targeting the IRE1α-XBP1 branch of the unfolded protein response in human diseases. Semin. Cancer Biol. *33*, 48–56.
8. Hotamisligil, G.S., and Davis, R.J. (2016). Cell signaling and stress responses. Cold Spring Harb. Perspect. Biol. *8*, a006072.
9. Kanda, S., Yanagitani, K., Yokota, Y., Esaki, Y., and Kohno, K. (2016). Autonomous translational pausing is required for XBP1u mRNA recruitment to the ER via the SRP pathway. Proc. Natl. Acad. Sci. USA *113*, E5886–E5895.
10. Guo, F., Lin, E.A., Liu, P., Lin, J., and Liu, C. (2010). XBP1U inhibits the XBP1S-mediated upregulation of the iNOS gene expression in mammalian ER stress response. Cell. Signal. *22*, 1818–1828.
11. Brozzi, F., Gerlo, S., Grieco, F.A., Juusola, M., Balhuizen, A., Lievens, S., Gysemans, C., Bugliani, M., Mathieu, C., Marchetti, P., et al. (2016). Ubiquitin D regulates IRE1α/c-Jun N-terminal kinase (JNK) protein-dependent apoptosis in pancreatic beta cells. J. Biol. Chem. *291*, 12040–12056.
12. Soustek, M.S., Balsa, E., Barrow, J.J., Jedrychowski, M., Vogel, R., Jan Smeitink, Gygi, S.P., and Puigserver, P. (2018). Inhibition of the ER stress IRE1α inflammatory pathway protects against cell death in mitochondrial complex I mutant cells. Cell Death Dis. *9*, 658.
13. Carter, R.J., and Parsons, J.L. (2016). Base excision repair, a pathway regulated by posttranslational modifications. Mol. Cell. Biol. *36*, 1426–1437.
14. Lee, M.J., and Yaffe, M.B. (2016). Protein regulation in signal transduction. Cold Spring Harb. Perspect. Biol. *8*, a005918.
15. Nadolski, M.J., and Linder, M.E. (2007). Protein lipidation. FEBS J. *274*, 5202–5210.
16. Globa, A.K., and Bamji, S.X. (2017). Protein palmitoylation in the development and plasticity of neuronal connections. Curr. Opin. Neurobiol. *45*, 210–220.
17. Mitchell, D.A., Vasudevan, A., Linder, M.E., and Deschenes, R.J. (2006). Protein palmitoylation by a family of DHHC protein *S*-acyltransferases. J. Lipid Res. *47*, 1118–1127.
18. Daniotti, J.L., Pedro, M.P., and Valdez Taubas, J. (2017). The role of S-acylation in protein trafficking. Traffic *18*, 699–710.
19. Korycka, J., Łach, A., Heger, E., Bogusławska, D.M., Wolny, M., Toporkiewicz, M., Augoff, K., Korzeniewski, J., and Sikorski, A.F. (2012). Human DHHC proteins: a spotlight on the hidden player of palmitoylation. Eur. J. Cell Biol. *91*, 107–117.

20. Ko, P.J., and Dixon, S.J. (2018). Protein palmitoylation and cancer. EMBO Rep. *19*, e46666.

21. Resh, M.D. (2017). Palmitoylation of proteins in cancer. Biochem. Soc. Trans. *45*, 409–416.

22. Chen, X., Ma, H., Wang, Z., Zhang, S., Yang, H., and Fang, Z. (2017). EZH2 palmitoylation mediated by ZDHHC5 in p53-mutant glioma drives malignant development and progression. Cancer Res. *77*, 4998–5010.

23. Chen, X., Hu, L., Yang, H., Ma, H., Ye, K., Zhao, C., Zhao, Z., Dai, H., Wang, H., and Fang, Z. (2019). DHHC protein family targets different subsets of glioma stem cells in specific niches. J. Exp. Clin. Cancer Res. *38*, 25.

24. Chen, X., Du, Z., Shi, W., Wang, C., Yang, Y., Wang, F., Yao, Y., He, K., and Hao, A. (2014). 2-Bromopalmitate modulates neuronal differentiation through the regulation of histone acetylation. Stem Cell Res. (Amst.) *12*, 481–491.

25. DeJesus, G., and Bizzozero, O.A. (2002). Effect of 2-fluoropalmitate, cerulenin and tunicamycin on the palmitoylation and intracellular translocation of myelin proteolipid protein. Neurochem. Res. *27*, 1669–1675.

26. Gruber, C.W., Cemazar, M., Heras, B., Martin, J.L., and Craik, D.J. (2006). Protein disulfide isomerase: the structure of oxidative folding. Trends Biochem. Sci. *31*, 455–464.

27. Ma, Y., and Hendershot, L.M. (2004). Herp is dually regulated by both the endoplasmic reticulum stress-specific branch of the unfolded protein response and a branch that is shared with other cellular stress pathways. J. Biol. Chem. *279*, 13792–13799.

28. Majumder, M., Huang, C., Snider, M.D., Komar, A.A., Tanaka, J., Kaufman, R.J., Krokowski, D., and Hatzoglou, M. (2012). A novel feedback loop regulates the response to endoplasmic reticulum stress via the cooperation of cytoplasmic splicing and mRNA translation. Mol. Cell. Biol. *32*, 992–1003.

29. Chen, H., and Qi, L. (2010). SUMO modification regulates the transcriptional activity of XBP1. Biochem. J. *429*, 95–102.

30. Lin, D.T.S., Davis, N.G., and Conibear, E. (2017). Targeting the Ras palmitoylation/depalmitoylation cycle in cancer. Biochem. Soc. Trans. *45*, 913–921.

31. Buglino, J.A., and Resh, M.D. (2012). Palmitoylation of Hedgehog proteins. Vitam. Horm. *88*, 229–252.

32. Janda, C.Y., and Garcia, K.C. (2015). Wnt acylation and its functional implication in Wnt signalling regulation. Biochem. Soc. Trans. *43*, 211–216.

33. Runkle, K.B., Kharbanda, A., Stypulkowski, E., Cao, X.J., Wang, W., Garcia, B.A., and Witze, E.S. (2016). Inhibition of DHHC20-mediated EGFR palmitoylation creates a dependence on EGFR signaling. Mol. Cell *62*, 385–396.

34. Jennings, B.C., Nadolski, M.J., Ling, Y., Baker, M.B., Harrison, M.L., Deschenes, R.J., and Linder, M.E. (2009). 2-Bromopalmitate and 2-(2-hydroxy-5-nitro-benzylidene)-benzo[*b*]thiophen-3-one inhibit DHHC-mediated palmitoylation in vitro. J. Lipid Res. *50*, 233–242.

35. Zheng, B., DeRan, M., Li, X., Liao, X., Fukata, M., and Wu, X. (2013). 2-Bromopalmitate analogues as activity-based probes to explore palmitoyl acyltransferases. J. Am. Chem. Soc. *135*, 7082–7085.

36. Resh, M.D. (2006). Use of analogs and inhibitors to study the functional significance of protein palmitoylation. Methods *40*, 191–197.

37. Zheng, B., Zhu, S., and Wu, X. (2015). Clickable analogue of cerulenin as chemical probe to explore protein palmitoylation. ACS Chem. Biol. *10*, 115–121.

38. Brown, M., Strudwick, N., Suwara, M., Sutcliffe, L.K., Mihai, A.D., Ali, A.A., Watson, J.N., and Schröder, M. (2016). An initial phase of JNK activation inhibits cell death early in the endoplasmic reticulum stress response. J. Cell Sci. *129*, 2317–2328.

39. Jurczak, M.J., Lee, A.H., Jornayvaz, F.R., Lee, H.Y., Birkenfeld, A.L., Guigni, B.A., Kahn, M., Samuel, V.T., Glimcher, L.H., and Shulman, G.I. (2012). Dissociation of inositol-requiring enzyme (IRE1α)-mediated c-Jun N-terminal kinase activation from hepatic insulin resistance in conditional X-box-binding protein-1 (XBP1) knock-out mice. J. Biol. Chem. *287*, 2558–2567.

40. Kishino, A., Hayashi, K., Hidai, C., Masuda, T., Nomura, Y., and Oshima, T. (2017). XBP1-FoxO1 interaction regulates ER stress-induced autophagy in auditory cells. Sci. Rep. *7*, 4442.

41. Dadey, D.Y.A., Kapoor, V., Khudanyan, A., Thotala, D., and Hallahan, D.E. (2018). PERK regulates glioblastoma sensitivity to ER stress although promoting radiation resistance. Mol. Cancer Res. *16*, 1447–1453.

42. Lhomond, S., Avril, T., Dejeans, N., Voutetakis, K., Doultsinos, D., McMahon, M., Pineau, R., Obacz, J., Papadodima, O., Jouan, F., et al. (2018). Dual IRE1 RNase functions dictate glioblastoma development. EMBO Mol. Med. *10*, e7929.

43. Xu, X., Liu, J., Huang, B., Chen, M., Yuan, S., Li, X., and Li, J. (2017). Reduced response of IRE1α/Xbp-1 signaling pathway to bortezomib contributes to drug resistance in multiple myeloma cells. Tumori *103*, 261–267.

44. Nicolao, M.C., Loos, J.A., Rodriguez Rodrigues, C., Beas, V., and Cumino, A.C. (2017). Bortezomib initiates endoplasmic reticulum stress, elicits autophagy and death in *Echinococcus granulosus* larval stage. PLoS ONE *12*, e0181528.

45. Gill, G. (2005). Something about SUMO inhibits transcription. Curr. Opin. Genet. Dev. *15*, 536–541.

46. Cheng, J., Wang, D., Wang, Z., and Yeh, E.T. (2004). SENP1 enhances androgen receptor-dependent transcription through desumoylation of histone deacetylase 1. Mol. Cell. Biol. *24*, 6021–6028.